Intracomplex CH_3OH Walking around Optically Active 1-Methyl-3-ethylallyl Cations. A Gas-Phase Kinetic Study

Anna Troiani and Maurizio Speranza*

Facoltà di Farmacia, Dipartimento di Studi di Chimica e Tecnologia delle Sostanze Biologicamente Attive, Università degli Studi di Roma "La Sapienza", P. le A. Moro 5, 00185 Rome, Italy

Received July 14, 1997

The kinetics and the mechanism of the racemization and regioisomerization of O-methylated (*S*)-*trans*-4-hexen-3-ol (**IS′**) or (*R*)-*trans*-3-hexen-2-ol (**IIR′**) have been investigated in the gas phase at 720 Torr and in the 40−120 °C temperature range. The starting oxonium intermediates were generated in the gas phase by the reaction of $(CH_3)_2Cl^+$ ions, formed by stationary γ-radiolysis of bulk CH_3Cl, on the corresponding optically active alcohols. The rate constant of the gas-phase regioisomerization of **IS′** ((3.4−16.0) × 10^6 s^{-1}) was found to exceed that of its racemization ((1.9−9.8) × 10^6 s^{-1}) over the entire temperature range. Similar differences were observed for the regioisomerization ((2.9−15.0) × 10^6 s^{-1}) and the racemization of **IIR′** ((1.8−9.6) × 10^6 s^{-1}). By analogy with previous experimental and theoretical evidence, these results are consistent with intramolecular racemization and regioisomerization processes involving the intermediacy of two distinct hydrogen-bonded complexes, wherein the CH_3OH molecule is coplanarly coordinated to the in-plane hydrogens of the 1-methyl-3-ethylallyl moiety. The activation parameters for their formation from the **IS′** and **IIR′** were evaluated and compared with those concerning the racemization and regioisomerization of O-protonated (*S*)-*trans*-4-hexen-3-ol (**IS**), previously measured in the gas phase under similar experimental conditions. The comparison reveals that gas-phase racemization and regioisomerization of O-protonated (*S*)-*trans*-4-hexen-3-ol (**1S′**) (AOH=H_2O) involve transition structures located early along the reaction coordinate, whereas the transition structures involved in the rearrangement of O-methylated (*S*)-*trans*-4-hexen-3-ol (**1S′**) and (*R*)-*trans*-3-hexen-2-ol (**IIR′**) (AOH = CH_3OH) are placed later along the reaction coordinate and are characterized by a strong coordination of the moving CH_3OH molecule with the hydrogens of the allylic moiety.

Introduction

In the preceding paper of this series,[1] the kinetics and the dynamics of the unimolecular racemization and regioisomerization of O-protonated (*S*)-*trans*-4-hexen-3-ol (the $\mathbf{IS}_{anti}/\mathbf{IS}_{syn}$ mixture in Scheme 1) have been investigated in the dilute gas state, i.e., in a reaction environment entirely free from the interference of solvation, ion-pairing, etc., that normally complicates analogous studies in solution.[2−9] The results are consistent with a gas-phase intramolecular racemization and regioisomerization involving the intermediacy of the hy-

Scheme 1

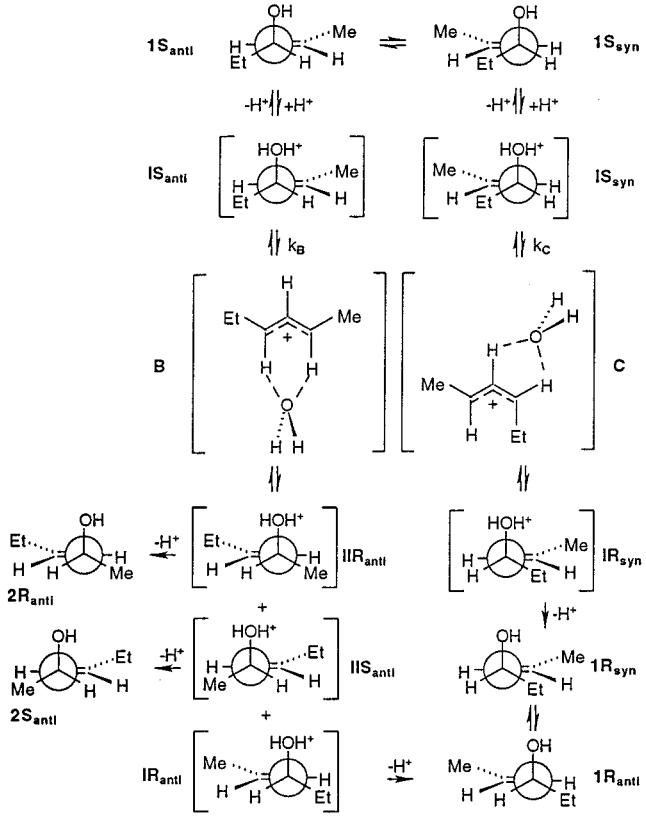

* To whom correspondence should be addressed. E-mail: speranza@axrma.uniromal.it.

(1) Chiral Ions in the Gas Phase. 2. Part 1: Troiani, A.; Gasparrini, F.; Grandinetti, F.; Speranza, M. *J. Am. Chem. Soc.* **1997**, *119*, 4525.

(2) For reviews, see: (a) Samuel, D.; Silver, B. *Adv. Phys. Org. Chem.* **1965**, *3*, 128. (b) Raber, D. J.; Harris, J. M.; Schleyer, P.v. R. *Ions and Ion Pairs in Organic Reactions*; Szwarc, M., Ed.; Wiley: New York, 1974; Vol. 2.

(3) Herlihy, K. P. *Aust. J. Chem.* **1982**, *35*, 2221.

(4) Allen, A. D.; Kanagasabapathy, V. D.; Tidwell, T. T. *J. Am. Chem. Soc.* **1984**, *106*, 1361.

(5) Dietze, P. E.; Jencks, W. P. *J. Am. Chem. Soc.* **1987**, *109*, 2057.

(6) Merritt, M. V.; Bronson, G. E.; Baczynskyj, L.; Boal, J. R. *J. Am. Chem. Soc.* **1980**, *102*, 346.

(7) Merritt, M. V.; Bell, S. J.; Cheon, H. J.; Darlington, J. A.; Dugger, T. L.; Elliott, N. B.; Fairbrother, G. L.; Melendez, C. S.; Smith, E. V.; Schwartz, P. L. *J. Am. Chem. Soc.* **1990**, *112*, 3560.

(8) Merritt, M. V.; Anderson, D. B.; Basu, K. A.; Chang, I. W.; Cheon, H. J.; Mukundan, N. E.; Flannery, C. A.; Kim, A. Y.; Vaishampayan, A.; Yens, D. A. *J. Am. Chem. Soc.* **1994**, *116*, 5551.

(9) (a) Thibblin, A. *J. Chem. Soc., Perkin Trans. 2* **1987**, 1987. (b) Thibblin, A. *J. Chem. Soc., Chem. Commun.* **1990**, 697. (c) Thibblin, A. *J. Chem. Soc., Perkin Trans. 2* **1992**, 1195.

S0022-3263(97)01282-6 CCC: $15.00
Published on Web 01/27/1998

drogen-bonded complexes **B** and **C** in Scheme 1.[10] Ab initio calculations on related model systems provided some insights into the nature of these complexes, wherein bonding between H_2O and the allyl cation residue is "site-specific", i.e., the relative orientation of the two moieties is locked by the favorable bonding interactions between several specific sites.[1,11] In the particular case of **B** and **C**, the moving H_2O molecule is coplanarly coordinated to the in-plane hydrogens of the allyl cation moiety. The formation of these hydrogen-bonded complexes is determined by kinetic factors as well as by the specific conformation of their oxonium ion precursors. Indeed, protonation of the $\mathbf{1S_{anti}}/\mathbf{1S_{syn}}$ mixture produces the two noninterconverting oxonium ion conformers $\mathbf{IS_{anti}}$ and $\mathbf{IS_{syn}}$ of Scheme 1. Conformer $\mathbf{IS_{syn}}$ evolves exclusively to its racemate (henceforth denoted by **1S−1R**) through complex **C**, whereas conformer $\mathbf{IS_{anti}}$ rearranges to complex **B** and eventually to the racemates of both the starting alcohol (**1S−1R**) and its isomer *trans*-3-hexen-2-ol (henceforth denoted by **2S−2R**, Scheme 1). Rearrangement of $\mathbf{IS_{anti}}$ and $\mathbf{IS_{syn}}$ to the corresponding complexes **B** and **C** involves activation energies of 7.4 ± 0.5 and 8.6 ± 0.6 kcal mol^{-1}, respectively. These findings, coupled with the theoretical evidence, point to transition structures wherein a significant fraction of the positive charge resides on the allylic moiety.

To enlarge our knowledge of the factors governing acid-promoted unimolecular racemization and regioisomerization of chiral allyl alcohols in the gaseous state, the kinetic investigation has been now extended to the rearrangement of (*S*)-*trans*-4-hexen-3-ol (the $\mathbf{1S_{anti}}/\mathbf{1S_{syn}}$ mixture, henceforth denoted as **1S**) and (*R*)-*trans*-3-hexen-2-ol (the $\mathbf{2R_{anti}}/\mathbf{2R_{syn}}$ mixture, henceforth denoted as **2R**) promoted by a pure Lewis acid, such as the dimethylchloronium ion $(CH_3)_2Cl^+$ (Scheme 2). By this approach, the methylated oxonium ions $\mathbf{IS'_{anti}}/\mathbf{IS'_{syn}}$ (henceforth denoted as **IS′**) and $\mathbf{IIR'_{anti}}/\mathbf{IIR'_{syn}}$ (henceforth denoted as **IIR′**) can be readily prepared in the dilute gas phase and their rearrangement kinetics evaluated with the same procedures employed in previous studies.[1] Thus, stationary concentrations of the $(CH_3)_2Cl^+$ Lewis acid have been generated from γ-radiolysis of gaseous mixtures, containing CH_3Cl, as the bulk component (720 Torr), together with traces of the chiral alcohol (either **1S** or **2R**; 0.5−0.7 Torr), of O_2, as a radical scavenger (10 Torr), and of $(CH_3O)_3PO$ (0.8−0.9 Torr), as a powerful base (proton affinity (PA)=212.0 kcal mol^{-1}).[12] Under such conditions, the high collisional frequency (ca. 10^{10} s^{-1}) with the bulk CH_3Cl molecules allows stabilization and thermal equilibration of **IS′** or **IIR′** prior to their rearrangement, whose course can be inferred from the yield and composition of their neutral rearranged products.

It is hoped that this study may provide some information on the course and the kinetics of the racemization and regioisomerization of the unsolvated isomeric intermediates **IS′** or **IIR′**. The comparison of the activation parameters governing their interconversion may prove the consistency of the kinetic methodology adopted and may elucidate the influence of the structure of the starting species. Finally, some insight into the role of the moving moiety (H_2O in Scheme 1; CH_3OH in Scheme 2) in determining the kinetics and the dynamics of the unimolecular rearrangement of the selected unsolvated oxonium ions may arise from a careful comparison with the results of the previous paper.

Scheme 2

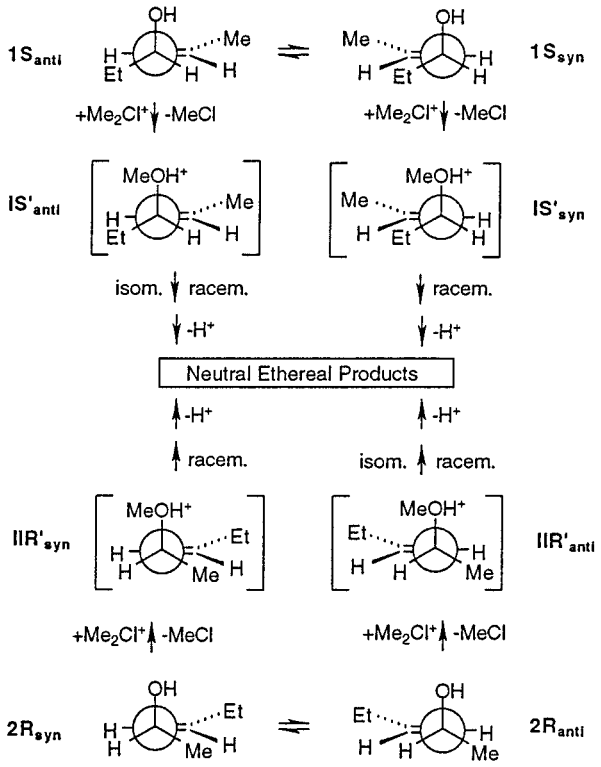

Experimental Section

Materials. Methyl choride and oxygen were high-purity gases from UCAR Specialty Gases N.V., used without further purification. $H_2{}^{18}O$ (^{18}O-content > 97%), CH_3OH, $(C_2H_5)_3N$, and $(CH_3O)_3PO$ were research grade chemicals from Aldrich Chemical Co. The racemates of (*S*,*R*)-*trans*-4-hexen-3-ol (**1S−1R**) and (*S*,*R*)-*trans*-3-hexen-2-ol (**2S−2R**) were prepared and purified according to previously described procedures.[1,13] The kinetic resolution of the **1S−1R** and **2S−2R** racemates was carried out by lipase-catalyzed enantioselective transesterification, using the same procedure employed in the previous paper.[1] The enantiomeric excess (ee) of the purified (*S*)-*trans*-4-hexen-3-ol (**1S**) and (*S*)-*trans*-3-hexen-2-ol (**2S**) was 98.5%; that of (*R*)-*trans*-4-hexen-3-ol (**1R**) and (*R*)-*trans*-3-hexen-2-ol (**2R**) was 99.0%. Their methyl ethers, i.e., (*S*)-*trans*-3-methoxy-4-hexene (**1S′**), (*R*)-*trans*-3-methoxy-4-hexene (**1R′**), (*S*)-*trans*-2-methoxy-3-hexene (**2S′**), and (*R*)-*trans*-2-methoxy-3-hexene (**2R′**) were synthesized from the corresponding chiral alcohols by well-established procedures.[14]

Procedure. The experimental techniques used for the preparation of the gaseous mixtures and their irradiation have been described previously.[1] The irradiations were carried out at a temperature ranging from 40 to 120 °C in a 220 Gammacell from Nuclear Canada Ltd. to a dose of 2×10^4 Gy at a rate of 10^4 Gy h^{-1}, as determined by a neopentane dosimeter. Control experiments, carried out at doses ranging from 1×10^4 to 1×10^5 Gy, showed that the relative yields of products are largely independent of the dose. The radiolytic products were analyzed by GLC, using a Perkin-Elmer 8700 gas chromatograph equipped with a flame ionization detector

(10) McAdoo, D. J.; Morton, T. H. *Acc. Chem. Res.* **1993**, *26*, 295.
(11) An outstanding example of site-specific interactions in ion−molecule complexes is given in: Sunner, J. A.; Hirao, K.; Kebarle, P. *J. Phys. Chem.* **1989**, *93*, 4010.
(12) Lias, S. G.; Bartmess, J. E.; Liebman, J. F.; Holmes, J. L.; Levin, R. D.; Mallard, W. G. *J. Phys. Chem. Ref. Data* **1988**, *17*, Suppl. 1.
(13) Coburn, E. R. *Organic Syntheses*; Wiley: New York, 1955; Collect. Vol. III, p 696.

Table 1. Relative Yields of the Methylated Products from the Gas-Phase Attack of $(CH_3)_2Cl^+$ Ions on 1S in the Presence of the Base $(CH_3O)_3PO$

system composition[a]		rctn temp	yield factors[b]			
1S (Torr)	$(CH_3O)_3PO$ (Torr)	(°C)	$Y_{\mathbf{1S'}}$	$Y_{\mathbf{1R'}}$	$Y_{\mathbf{2R'}}$	$Y_{\mathbf{2S'}}$
0.59	0.90	40	0.909	0.033	0.029	0.029
0.60	0.90	70	0.825	0.068	0.053	0.054
0.59	0.90	100	0.695	0.114	0.096	0.095
0.60	0.83	120	0.434	0.226	0.170	0.170

[a] CH_3Cl: 720 Torr; O_2: 4 Torr. Radiation dose 2×10^4 Gy (dose rate: 1×10^4 Gy h^{-1}). [b] Expressed as the ratio Y_M = [methylated product M]/Σ[methylated products] (see text). Each value is the average of several determinations, with an uncertainty level of ca. 5%.

Table 2. Relative Yields of the Methylated Products from the Gas-Phase Attack of $(CH_3)_2Cl^+$ Ions on 2R in the Presence of the Base $(CH_3O)_3PO$

system composition[a]		rctn temp	yield factors[b]			
2R (Torr)	$(CH_3O)_3PO$ (Torr)	(°C)	$Y_{\mathbf{2R'}}$	$Y_{\mathbf{2S'}}$	$Y_{\mathbf{1R'}}$	$Y_{\mathbf{1S'}}$
0.55	0.84	40	0.913	0.033	0.027	0.027
0.54	0.89	70	0.830	0.065	0.052	0.053
0.73	0.88	85	0.681	0.125	0.098	0.096
0.72	0.90	100	0.620	0.150	0.115	0.115
0.75	0.91	120	0.495	0.205	0.150	0.150

[a] CH_3Cl: 720 Torr; O_2: 4 Torr. Radiation dose 2×10^4 Gy (dose rate: 1×10^4 Gy h^{-1}}. [b] Expressed as the ratio Y_M = [methylated product M]/Σ[methylated products] (see text). Each value is the average of several determinations, with an uncertainty level of ca. 5%.

(FID), on a 25 m long, 0.25 mm i.d. MEGADEX 5 (30% dimethylpentyl-β-cyclodextrin in OV 1701) fused silica column, operated at temperatures ranging from 40 to 65 °C, 3 °C min^{-1}. The products were identified by comparison of their retention volumes with those of authentic standard compounds and their identity checked by GLC−MS, using a Hewlett-Packard 5890 A gas chomatograph in line with a HP 5970 B mass-selective detector. Their yields were determined from the areas of the corresponding eluted peaks, using the internal standard (i.e., 3-methylpentan-3-ol) method and individual calibration factors to correct for the detector response. Blank experiments were carried out to ascertain the occurrence and the extent of thermal isomerization and racemization of the individual starting substrates, i.e., **1S** and **2R**, as well as of their methyl ethers at any given reaction temperature. The yields of the radiolytic products from $(CH_3)_2Cl^+$-methylation of **1S** and **2R** were corrected accordingly.

Results

Gas-phase γ-radiolysis of gaseous mixtures containing CH_3Cl, as the bulk gas, together with traces of the base B = $(CH_3O)_3PO$ and of either (*S*)-*trans*-4-hexen-3-ol (**1S**) or (*R*)-*trans*-3-hexen-2-ol (**2R**), yields the corresponding methylated derivatives, namely (*S*)-*trans*-3-methoxy-4-hexene (**1S′**), (*R*)-*trans*-3-methoxy-4-hexene (**1R′**), (*S*)-*trans*-2-methoxy-3-hexene (**2S′**), and (*R*)-*trans*-2-methoxy-3-hexene (**2R′**), as the only detectable methylation products. These methylated derivatives are invariably accompanied by higher amounts of the corresponding chloromethylated derivatives. Other conceivable products, such as the cis isomers of the above ethers and the enantiomer of the starting alcohol and its isomers were not found in the mixtures irradiated under all experimental conditions. The absolute yields of the alkylated products, expressed as the number of molecules M produced per 100 eV of energy absorbed by the gaseous mixture (*G*(M) values), were measured under various experimental conditions, at temperatures from 40 to 120 °C and for a total dose of 2×10^4 Gy (dose rate: 1×10^4 Gy h^{-1}). For both starting substrates, the *G*(M) values of the methylated products range from 0.2 to 0.5, whereas those of the chloromethylated derivatives range from 0.5 to 1.6. A drastic decrease of these *G*(M) values (by over 85%) is observed by replacing $(CH_3O)_3PO$ (0.1 mol %) with 0.4 mol % of the very strong $(C_2H_5)_3N$ base.

Table 1 shows the composition of the irradiated mixtures and the relative distribution of the methylated products formed from the gas-phase methylation of **1S** in the presence of the base B = $(CH_3O)_3PO$. The results concerning the systems with **2R**, as the substrate, are listed in Table 2.

Ancillary experiments have been carried out under the conditions comparable to those of Tables 1 and 2 to gain some indirect pieces of information about the relative stability of the **IS′-IR′** and **IIS′-IIR′** oxonium racemates. Thus, free *exo*-1-methyl-*exo*-3-ethylallyl cations have been generated in 720 Torr of CH_4 at 40−120 °C by radiolytic protonation of *trans*,*trans*- or *cis*,*trans*-2,4-hexadiene (0.5−0.7 Torr) in the presence of ca. 1 Torr of CH_3OH. These free allyl cations were found to efficiently add to CH_3OH, yielding approximately equal amounts of **1S′**−**1R′** (53%) and **2S′**−**2R′** (47%) in absolute yields slightly decreased by increasing the temperature (overall *G*(M) = 1.2). Again, no formation of the corresponding cis isomers was observed.

Another set of experiments was aimed at verifying the role of the ubiquitous H_2O impurity, originally present in the gaseous samples or formed from their irradiation. Thus, 0.8−0.9 Torr of the selected starting substrates **1S** and **2R** have been mixed with 720 of CH_3Cl, containing ca. 0.9 Torr of the base B = $(CH_3O)_3PO$ and ca. 1.4 Torr of deliberately added $H_2{}^{18}O$ (^{18}O-content >97%). Irradiation of these mixtures at 40−120 °C gives rise to the expected amounts of the ethereal products **1S′**−**1R′** and **2S′**−**2R′**. Their ^{18}O-content, as determined by mass spectrometry from the relative abundances of their $[M - 29]^+$ (m/z = 85(^{16}O); 87(^{18}O)) and $[M - 15]^+$ (m/z = 99(^{16}O); 101(^{18}O)) fragments, was found to be below 5%, irrespective of irradiation temperature.

Discussion

Nature of the Ionic Reagents. Ionization of gaseous CH_3Cl is known to generate both $(CH_3)_2Cl^+$ and CH_2Cl^+ ions as the final ionic species completely unreactive toward their neutral precursor.[15−21] Thermal $(CH_3)_2Cl^+$ ($\Delta H_f°$ = 184 kcal mol^{-1})[12,22] behaves as a pure Lewis acid

(14) Vogel, A. *Textbook of Practical Organic Chemistry*; Langman Group Limited: Chapter IIIG, p 413.
(15) Luczynsky, Z.; Herman, J. A. *J. Phys. Chem.* **1978**, *82*, 1679.
(16) Benezra, S. A.; Hoffman, M. K.; Bursey, M. M. *J. Am. Chem. Soc.* **1970**, *92*, 7501.
(17) Pabst, M. J. K.; Tan, H. S.; Franklin, J. L. *Int. J. Mass Spectrom. Ion Phys.* **1976**, *20*, 191.
(18) Blint, R. J.; McMahon, T. B.; Beauchamp, J. L. *J. Am. Chem. Soc.* **1974**, *96*, 1269.
(19) Beauchamp, J. L.; Holtz, D.; Woodgate, S. D.; Patt, S. L. *J. Am. Chem. Soc.* **1972**, *94*, 2798.
(20) Holtz, D.; Beauchamp, J. L.; Woodgate, S. D. *J. Am. Chem. Soc.* **1970**, *92*, 7484.
(21) Herod, A. A.; Harrison, A. G.; McAskill, N. A. *Can. J. Chem.* **1971**, *49*, 2217.
(22) (a) Glukhovtsev, M. N.; Szulejko, J. E.; McMahon, T. B.; Gauld, J. W.; Scott, A. P.; Smith, B. J.; Pross, A.; Radom, L. *J. Phys. Chem.* **1994**, *98*, 13099. (b) McMahon, T. B.; Heinis, T.; Nicol, G.; Hovey, J. K.; Kebarle, P. *J. Am. Chem. Soc.* **1988**, *110*, 7591.

Scheme 3

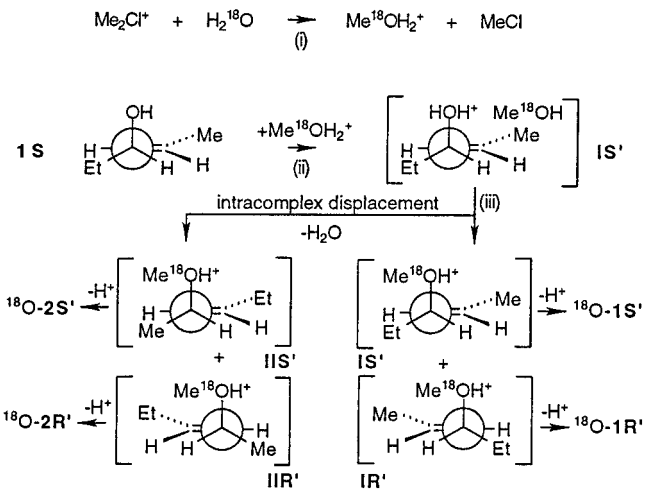

with a distinct affinity for n-type nucleophiles.[23−28] The allylic substrate **1S** or **2R** (0.07−0.10 mol %) and the base B = $(CH_3O)_3PO$ (0.11−0.12 mol %) are n-type nucleophiles deliberately added to the gaseous systems, which however contain also H_2O as an ubiquitous impurity either initially introduced in the mixture together with its bulk components or formed from its radiolysis. As pointed out in the previous paper,[1] the average stationary concentration of H_2O in the radiolytic systems is estimated to approach the combined concentration of the added n-type nucleophiles. Thus, taking into account the relatively high diffusion rate of H_2O in the gaseous medium, a significant fraction of the radiolytic $(CH_3)_2Cl^+$ ions is expected to be trapped by H_2O, yielding inter alia $CH_3OH_2^+$ (i in Scheme 3). The fate of this ion in the radiolytic mixtures is determined by the nature and the concentration of the other n-type nucleophile. Unless neutralized by $(CH_3O)_3PO$, it may exothermically transfer a proton to the allylic alcohol yielding its O-protonated derivative (either **IS** or **IIR**) and CH_3OH (ii in Scheme 3).[29] In this case, an ion−neutral complex between the O-protonated allylic alcohol (**IS** or **IIR**) and CH_3OH may be formed, wherein an intracluster nucleophilic CH_3OH-to-H_2O displacement might take place,[29] yielding eventually the same ethers of Tables 1 and 2 and H_2O (eq iii in Scheme 3).[30]

It is concluded that the ethereal products of Tables 1 and 2 may conceivably arise from two different routes: one induced by direct methylation of the allylic substrate from the radiolytic $(CH_3)_2Cl^+$ ions and the other promoted by preliminary proton transfer from $CH_3OH_2^+$ to the substrate followed by intracluster CH_3OH-to-H_2O displacement (sequence i → ii → iii in Scheme 3). This latter conceivable process is expected to generate a distribution of O-methylated allylic alcohols totally different from that arising from the first pathway. Since we are interested in investigating the gas-phase intramolecular racemization and isomerization reactions in the oxonium intermediate **IS′** and **IIR′**, it is crucial to recognize unequivocally the origin of radiolytic ethereal products of Tables 1 and 2, namely the relative contribution to their yields of the reaction pathways depicted in Schemes 2 and 3.

Nature of the Ethereal Products. The experimental conditions adopted in the present experiments, characterized by the low concentration of the allylic substrate (<0.1 mol %) diluted with a large excess of CH_3Cl, exclude direct radiolysis of the starting compound as a significant route to its alkylated products. Occurrence of possible free-radical pathways in the irradiated samples is strongly inhibited by the presence of an efficient thermal radical scavenger, such as oxygen, which does not interfere with the competing ionic processes, whose role is testified by the marked depressing effect of ca. 0.4 mol % of the powerful ion trap $(C_2H_5)_3N$ (PA = 232.3 kcal mol^{-1})[12] on the alkylated product yields.

The relative contribution of the reaction pathways of Schemes 2 and 3 to the ethereal products of Tables 1 and 2 is readily evaluated by measuring the extent of ^{18}O-incorporation into the radiolytic products after addition to the gaseous samples of an adequate concentration of $H_2{}^{18}O$ (^{18}O-content > 97%) (ca. 1.4 Torr). As reported in the Results, careful mass spectrometric analyses reveal that the ^{18}O-content in the methylated products **1S′**−**1R′** and **2S′**−**2R′** recovered in these systems never exceeds 5%, irrespective of the irradiation temperature (40−120 °C), thus pointing to the negligible contribution of sequence i → ii → iii of Scheme 3 to the formation of the ethereal products of Tables 1 and 2. It is concluded that these products arise predominantly from unimolecular racemization and regioisomerization of the primary oxonium intermediates, i.e., either **IS′** or **IIR′**, generated, respectively, from attack of the radiolytic methylating ions[30] on the selected substrates **1S** and **2R** (Scheme 2).

On these grounds, the yield factors Y_M of Tables 1 and 2 express the extent of racemization and regioisomerization of the primary oxonium intermediates **IS′** or **IIR′**, respectively. Taking into account that exothermic proton transfer from gaseous Brønsted acids, including the oxonium ions of Schemes 1 and 2, to powerful bases, such as B = $(CH_3O)_3PO$, is generally fast, the first-order rate constants for the formation of **1R′** ($k_{\mathbf{1R'}}$) and **2S′**−**2R′** ($k_{\mathbf{2S'-2R'}}$) from **IS′** at any given temperature can be expressed by $k_{\mathbf{1R'}} = t_{rctn}^{-1} \ln(1 - Y_{\mathbf{1R'}})^{-1}$ and $k_{\mathbf{2S'-2R'}} =$

(23) Speranza, M.; Pepe, N.; Cipollini, R. *J. Chem. Soc., Perkin Trans. 2* **1979**, 1179.
(24) Pepe, N.; Speranza, M. *J. Chem. Soc., Perkin Trans. 2* **1981**, 1430.
(25) Speranza, M.; Angelini, G. *J. Am. Chem. Soc.* **1980**, *102*, 3115.
(26) Angelini, G.; Speranza, M. *J. Am. Chem. Soc.* **1981**, *103*, 3792.
(27) Angelini, G.; Speranza, M. *J. Am. Chem. Soc.* **1981**, *103*, 3800.
(28) Colosimo, M.; Bucci, R. *J. Phys. Chem.* **1979**, *83*, 1952.
(29) Exact determination of the thermochemistry of these processes is presently inaccessible, owing to the lack of experimental thermochemical data for the ionic species involved. An approximate estimate of the PA of **1S** and **2R** (ca. 204 kcal mol^{-1}) can be obtained from a correlation between the ionization energies and the proton affinities of alcohols (ref 12). According to refs 12 and 22, the corresponding methyl cation affinity can be estimated to range around 100 kcal mol^{-1}. Thus, CH_3OH-to-H_2O nucleophilic displacement on **IS** and **IIR** is estimated to be ca. 9 kcal mol^{-1} exothermic. Proton transfer from $CH_3OH_2^+$ to the oxygen atom of **1S** and **2R** is calculated to be ca. 23 kcal mol^{-1} exothermic. The heat of formation of the 3-hydroxyhexan-4-yl and 2-hydroxyhexan-3-yl cations, hypothetically formed by proton transfer from $CH_3OH_2^+$ to the π-bond of **1S** and **2R**, is estimated by means of a modified isodesmic substitution to amount to ca. 140 kcal mol^{-1} (Bowen, R. D.; Williams, D. H. *J. Am. Chem. Soc.* **1978**, *100*, 7454). This corresponds to a site PA value for the π-bond of **1S** and **2R** of ca. 176 kcal mol^{-1}. Accordingly, proton transfer from $CH_3OH_2^+$ to the π bond of **1S** and **2R** is calculated to be endothermic by ca. 6 kcal mol^{-1}. On the grounds of the standard heats of formation of the **1S** and **2R** alcohols ($\Delta H_f°$ = ca. −49 kcal mol^{-1}) and of their methyl ethers ($\Delta H_f°$ = ca. −44 kcal mol^{-1}), estimated according to the group additivity method (Benson, S. W. *Thermochemical Kinetics*; Wiley: New York, 1968), O-methylation of **1S** and **2R** by $(CH_3)_2Cl^+$ is calculated to be ca. 42 kcal mol^{-1} exothermic.

(30) Alternatively, $CH_3OH_2^+$ may undergo a ca. 32 kcal mol^{-1} exothermic (ref 29) nucleophilic displacement of the H_2O molecule by the allylic alcohol. However, this conceivable process cannot be distinguished from direct methylation of the same substrate by $(CH_3)_2Cl^+$, since both lead to the same oxonium intermediate.

Table 3. Rate Constants of Intramolecular Racemization and Isomerization of IS′

	rctn extent[a]			rate constants ($\times 10^{-6}$ s^{-1})			
rctn temp (°C)	$Y_{\mathbf{1R'}}$	$Y_{\mathbf{2R'-2S'}}$	rctn time[b] t_{rctn}($\times 10^8$ s)	$k_{\mathbf{1R'}}$[c]	$k_{\mathbf{2R'-2S'}}$[c]	$k_{\mathbf{C^I}}$[d]	$k_{\mathbf{B^I}}$[e]
40	0.033	0.058	1.8	1.9	3.4	0.5 (5.66)	7.0 (6.84)
70	0.068	0.107	2.0	3.5	5.7	1.5 (6.17)	12.1 (7.08)
100	0.114	0.191	2.2	5.4	9.5	1.7 (6.24)	21.6 (7.33)
120	0.226	0.340	2.6	9.8	16.0	4.6 (6.66)	43.8 (7.64)

[a] See footnote b of Table 1. [b] Reaction time, t_{rctn}, calculated from the reciprocal of the first-order collision constant between **IS′** and $(CH_3O)_3PO$ (see text). [c] $k = t_{rctn}^{-1} \ln(1 - Y_M)^{-1}$ (see text). [d] $k_{\mathbf{C^I}} = t_{rctn}^{-1} \ln[1 - 2(Y_{\mathbf{1R'}} - 0.5Y_{\mathbf{2R'-2S'}})]^{-1}$ (see text), log $k_{\mathbf{C^I}}$ in parentheses. [e] $k_{\mathbf{B^I}} = t_{rctn}^{-1} \ln(1 - 2Y_{\mathbf{2R'-2S'}})^{-1}$ (see text), log $k_{\mathbf{B^I}}$ in parentheses.

Table 4. Rate Constants of Intramolecular Racemization and Isomerization of IIR′

	rctn extent[a]			rate constants ($\times 10^{-6}$ s^{-1})			
rctn temp (°C)	$Y_{\mathbf{2S'}}$	$Y_{\mathbf{1R'-1S'}}$	rctn time[b] t_{rctn}($\times 10^8$ s)	$k_{\mathbf{2S'}}$[c]	$k_{\mathbf{1R'-1S'}}$[c]	$k_{\mathbf{C^{II}}}$[d]	$k_{\mathbf{B^{II}}}$[e]
40	0.033	0.054	1.9	1.8	2.9	0.6 (5.80)	6.0 (6.78)
70	0.065	0.105	2.0	3.3	5.5	1.2 (6.10)	11.7 (7.07)
85	0.125	0.194	2.2	6.1	9.9	2.6 (6.42)	22.7 (7.36)
100	0.150	0.230	2.2	7.3	11.7	3.2 (6.51)	27.6 (7.44)
120	0.205	0.300	2.4	9.6	15.0	4.9 (6.69)	38.5 (7.58)

[a] See footnote b of Table 1. [b] Reaction time, t_{rctn}, calculated from the reciprocal of the first-order collision constant between **IIR′** and $(CH_3O)_3PO$ (see text). [c] $k = t_{rctn}^{-1} \ln(1 - Y_M)^{-1}$ (see text). [d] $k_{\mathbf{C^{II}}} = t_{rctn}^{-1} \ln[1 - 2(Y_{\mathbf{2S'}} - 0.5Y_{\mathbf{1R'-1S'}})]^{-1}$ (see text), log $k_{\mathbf{C^{II}}}$ in parentheses. [e] $k_{\mathbf{B^{II}}} = t_{rctn}^{-1} \ln(1 - 2Y_{\mathbf{1R'-1S'}})^{-1}$ (see text), log $k_{\mathbf{B^{II}}}$ in parentheses.

$t_{rctn}^{-1} \ln(1 - Y_{\mathbf{2S'-2R'}})^{-1}$, with t_{rctn} corresponding to the collision interval of **IS′** with the base B,[31] under the assumption that the trapping reaction occurs with unit efficiency. The relevant results are listed in Table 3. In the same way, the first-order rate constants for the formation of **2S′** ($k_{\mathbf{2S'}}$) and **1S′−1R′** ($k_{\mathbf{1S'-1R'}}$) from **IIR′** at any given temperature can be expressed by $k_{\mathbf{2S'}} = t_{rctn}^{-1} \ln(1 - Y_{\mathbf{2S'}})^{-1}$ and $k_{\mathbf{1S'-1R'}} = t_{rctn}^{-1} \ln(1 - Y_{\mathbf{1S'-1R'}})^{-1}$, with t_{rctn} corresponding to the collision interval of **IIR′** with the base B,[31] under the assumption that the trapping reaction occurs with unit efficiency. The relevant results are listed in Table 4.

The Regioisomerization and Racemization Mechanisms. Inspection of Tables 1 and 2 reveals that methylation of **1S** leads to [**1S′−1R′**]/[**2S′−2R′**] ratios ([**1S′−1R′**]/[**2S′−2R′**] = 1.14−1.33) that are substantially different from those obtained, under the same experimental conditions, from methylation of **2R** ([**1S′−1R′**]/[**2S′−2R′**]= 0.73−0.92). This observation, coupled with the [**1S′−1R′**]/[**2S′−2R′**] = 1.12 distribution obtained from addition of free *exo*-1-methyl-*exo*-3-ethylallyl cations on CH_3OH, indicates that, at any temperature, intramolecular rearrangement of **IS′** and **IIR′** must involve more than one distinct intermediate. The conceivable hypothesis that any of these intermediates may resemble Audier's [C_6H_{10}•$CH_3OH_2^+$] ion−molecule β-complexes[32] can be safely disregarded owing to the unfavorable proton affinity gap between hexadienes (PA > 202 kcal mol^{-1})[12] and methanol (PA = 181.9 kcal mol^{-1}).[12] Thus, the formation of the isomerization and racemization products of Tables 1 and 2 requires the intermediacy of distinct [$C_6H_{11}^+$•CH_3OH] complexes.

Concerning their nature, the formation of racemic products in Tables 1 and 2 suggests the intermediacy of structures wherein the CH_3OH molecule resides coplanarly to the $C_6H_{11}^+$ plane. Furthermore, at least one of these structures must involve site-specific interactions between CH_3OH and $C_6H_{11}^+$ favoring rebonding of the CH_3OH molecule at its original departure site with formation of the trans ethereal racemate (internal return). On these grounds and by analogy with previous experimental and theoretical evidence on related systems,[1] we are inclined to assign the hydrogen-bonded structure $\mathbf{C^I}$ (or $\mathbf{C^{II}}$) to this intermediate (Scheme 4). Besides, formation of the isomerization trans products in yields comparable to the racemization ones (Tables 1 and 2) points to a regioisomerization intermediate characterized by coplanarity between *trans,trans*-$C_6H_{11}^+$ and CH_3OH, which are held together by interactions similar to those operating in the hydrogen-bonded structure $\mathbf{C^I}$ (or $\mathbf{C^{II}}$). On these grounds and by analogy with previous experimental and theoretical evidence on related systems,[1] we are inclined to assign the hydrogen-bonded structure $\mathbf{B^I}$=$\mathbf{B^{II}}$ to this intermediate (vide infra). In the complex $\mathbf{C^I}$ (or $\mathbf{C^{II}}$), involved in the racemization of $\mathbf{IS'_{syn}}$ (or $\mathbf{IIR'_{syn}}$) (Scheme 4), equal is the probability that the CH_3OH moiety rebonds to the original side of the orbital (internal return to $\mathbf{IS'_{syn}}$ (or $\mathbf{IIR'_{syn}}$)) or moves to the other side, yielding the enantiomer $\mathbf{IR'_{syn}}$ (or $\mathbf{IIS'_{syn}}$). In the complex $\mathbf{B^I}$ (=$\mathbf{B^{II}}$), occurring in the rearrangement of $\mathbf{IS'_{anti}}$ (or $\mathbf{IIR'_{anti}}$), rebonding of CH_3OH to the allylic carbons would yield both the $\mathbf{IS'_{anti}}$−$\mathbf{IR'_{anti}}$ and $\mathbf{IIS'_{anti}}$−$\mathbf{IIR'_{anti}}$ racemates, in proportions depending on the corresponding activation free energies.[33]

Determination of the activation parameters governing unimolecular rearrangement of the primary oxonium intermediate **IS′** from O-methylation of **1S** requires an estimate of the relative extent of the competing conversions of intermediate $\mathbf{B^I}$=$\mathbf{B^{II}}$ to the $\mathbf{IS'_{anti}}$−$\mathbf{IR'_{anti}}$ and

(31) The reaction time, t_{rctn}, is taken as the inverse of the first-order collision rate constant $k' = k''$[$(MeO)_3PO$] between **IS′** (or **IIR′**) and the $(MeO)_3PO$ base, with the collision rate constant k'' calculated according to: Su, T.; Chesnavitch, W. J. *J. Chem. Phys.* **1982**, *76*, 5183. (k'' ($\times 10^9$ cm^3 molecule^{-1} s^{-1}) = 2.04 (40 °C); 1.97 (70 °C); 1.94 (85 °C); 1.92 (100 °C); 1.88 (120 °C)).

(32) (a) Audier, H. E.; Monteiro, C.; Berthomieu, D.; Tortajada, J. *Int. J. Mass Spectrom. Ion Proc.* **1991**, *104*, 145. (b) Audier, H. E.; Berthomieu, D.; Morton, T. H. *J. Org. Chem.* **1995**, *60*, 7198.

(33) Alternative hypothesis for intramolecular isomerization, such as that based on the complete racemization of the starting **IS′** to **IS′−IR′**, followed by the slow **IS′−IR′** → **IIS′−IIR′** regioisomerization, contrasts with the limited racemization ($Y_{\mathbf{1R'}}$; Table 1) and isomerization yield factors ($Y_{\mathbf{2R'-2S'}}$; Table 1) measured under all experimental conditions and with the observed increase of their ratio with temperature. The same trend excludes the possibility of slow isomerization of the starting **IS′** to **IIR′**, followed by fast **IIR′** → **IIS′** racemization. Analogous arguments apply in regard to the **IIR′** racemization and regioisomerization pathways.

Scheme 4

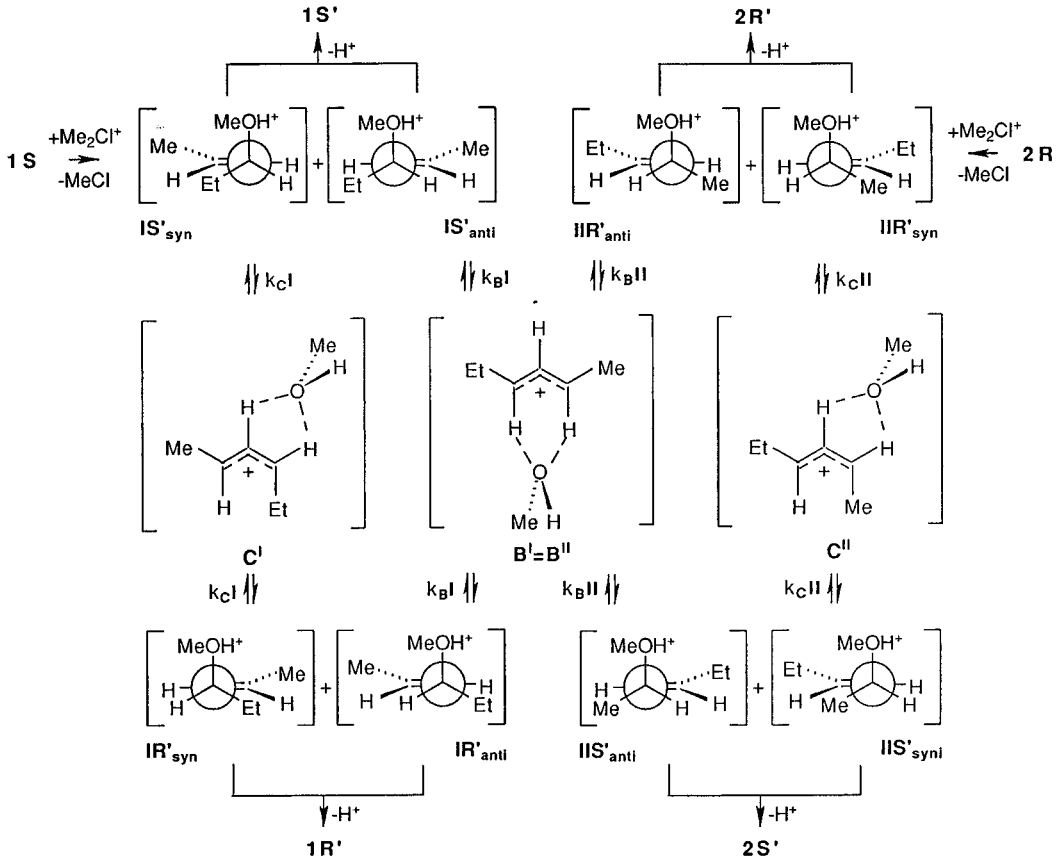

IIS′$_{anti}$−IIR′$_{anti}$ racemates. A way is to consider the **1S′**−**1R′** (53%) and **2S′**−**2R′** (47%) distribution from addition of free *exo*-1-methyl-*exo*-3-ethylallyl cations to CH_3OH as an evidence of essentially equal stability for their oxonium precursors **IS′**−**IR′** and **IIR′**−**IIS′**. Thereby, following the Hammond postulate, approximately equal free energy activation barriers can be expected for the conversion of **B^{I}=B^{II}** into the **IS′**−**IR′** and **IIR′**−**IIS′** intermediates. Along this line, the contribution of complex **B^{I}=B^{II}** to the **IS′** → **IR′** process is taken equal to one-half of the combined **2S′**−**2R′** isomerization yield (i.e., $0.5Y_{\mathbf{2R'-2S'}}$). Obviously, the contribution of complex **C^{I}** to the **IS′** → **IR′** process is calculated from $Y_{\mathbf{1R'}}-0.5Y_{\mathbf{2R'-2S'}}$. As a consequence, the formation rate of the **B^{I}=B^{II}** complex from **IS′** can be expressed by $k_{\mathbf{B^I}} = t_{rctn}^{-1} \ln(1 - 2Y_{\mathbf{2R'-2S'}})^{-1}$. Besides, considering equal the probability of conversion of the **C^{I}** structure into the **IR′** and **IS′** (internal return) enantiomers, the formation rate of the **C^{I}** complex from **IS′** is expressed by $k_{\mathbf{C^I}} = t_{rctn}^{-1} \ln[1 - 2(Y_{\mathbf{1R'}} - 0.5Y_{\mathbf{2R'-2S'}})]^{-1}$. The values of the $k_{\mathbf{B^I}}$ and $k_{\mathbf{C^I}}$ rate constants, obtained in the 40−120 °C range, are listed in Table 3. The corresponding Arrhenius plots are shown in Figure 1. Regression analysis of the data of Figure 1 leads to the following equations: $\log k_{\mathbf{B^I}} = (10.6 \pm 0.4) - [(5.4 \pm 0.5) \times 10^3]/2.303RT$ ($r = 0.978$) and $\log k_{\mathbf{C^I}} = (10.1 \pm 0.4) - [(6.3 \pm 0.5) \times 10^3]/2.303RT$ ($r = 0.960$).

Obviously, the same arguments apply, mutatis mutandis, to the **IIR′** racemization and regioisomerization pathways. The contribution of complex **B^{I}=B^{II}** to the **IIR′** → **IIS′** process is taken equal to one-half of the combined **1S′**−**1R′** isomerization yield (i.e., $0.5Y_{\mathbf{1R'-1S'}}$). Obviously, the contribution of complex **C^{II}** to the **IIR′** → **IIS′** process is calculated from $Y_{\mathbf{2S'}} - 0.5Y_{\mathbf{1R'-1S'}}$. As a consequence, the formation rate of the **B^{II}** complex from

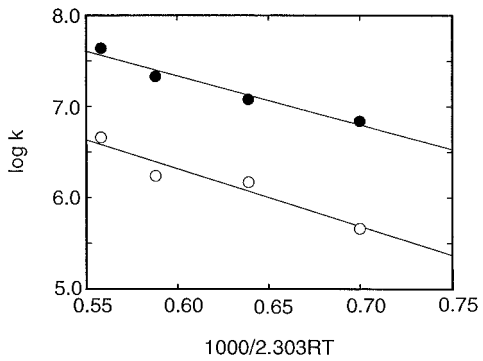

Figure 1. Arrhenius plot for the **IS′** → **B^{I}** (full circles) and **IS′** → **C^{I}** (open circles) intramolecular rearrangements in CH_3Cl (720 Torr).

IIR′ can be expressed by $k_{\mathbf{B^{II}}} = t_{rctn}^{-1} \ln(1 - 2Y_{\mathbf{1R'-1S'}})^{-1}$. Similarly, considering equal the probability of conversion of the **C^{II}** structure into the **IIS′** and **IIR′** (internal return) enantiomers, the formation rate of the **C^{II}** complex from **IIR′** is expressed by $k_{\mathbf{C^{II}}} = t_{rctn}^{-1} \ln[1 - 2(Y_{\mathbf{2S'}} - 0.5Y_{\mathbf{1R'-1S'}})]^{-1}$. The values of the $k_{\mathbf{B^{II}}}$ and $k_{\mathbf{C^{II}}}$ rate constants, obtained in the 40−120 °C range, are listed in Table 4. The corresponding Arrhenius plots are shown in Figure 2. Regression analysis of the data of Figure 2 leads to the equations: $\log k_{\mathbf{B^{II}}} = (10.9 \pm 0.4) - [(5.8 \pm 0.5) \times 10^3]/2.303RT$ ($r = 0.987$) and $\log k_{\mathbf{C^{II}}} = (10.3 \pm 0.4) - [(6.5 \pm 0.6) \times 10^3]/2.303RT$ ($r = 0.988$).

Comparison with Related Gas-Phase Studies. The Arrhenius equations for the gas-phase intramolecular racemization and regioisomerization of thermal oxonium intermediates **IS′** and **IIR′**, as derived from the corresponding data of Figures 1 and 2, are summarized

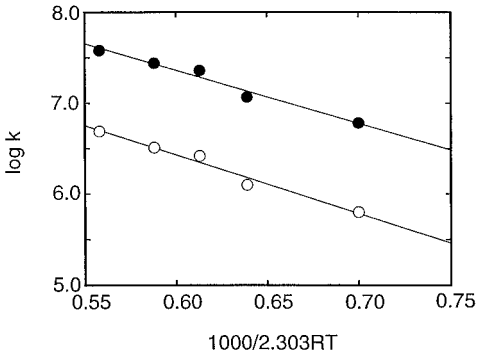

Figure 2. Arrhenius plot for the **IIR′** → **B^{II}** (full circles) and **IIR′** → **C^{II}** (open circles) intramolecular rearrangements in CH_3Cl (720 Torr).

in Table 5, together with those concerning the gas-phase intramolecular racemization and regioisomerization of the oxonium intermediate **IS** (Scheme 1). The relevant activation parameters, calculated from the transition-state theory equation, are reported as well, whose comparison corroborates the occurrence of two distinct reaction intermediates with site-specific hydrogen bonding, i.e., **B^{I}**=**B^{II}** and **C^{I}** (or **C^{II}**) (vide supra). Indeed, the activation parameters of Table 5 indicate that the **IS′** (and **IIR′**) racemization and regioisomerization must proceed through ion−molecule intermediates having comparable dissociation energy above ca. 13 kcal mol^{-1}, namely the energy typical of gas-phase C−H···O hydrogen-bond interactions.[34,35]

Inspection of the kinetic parameters of Table 5 reveals the following: (i) an inverse correlation does exist between the C−O bond dissociation energies of the allylic oxonium intermediates (BE) and $\Delta H^{\ddagger}$'s by varying the nature of the migrating AOH (A = H or CH_3) moiety. Indeed, $\Delta H^{\ddagger}$'s for rearrangement of **IS′** and of **IIR′** (AOH = CH_3OH; BE = 19 kcal mol^{-1}) are ca. 2 kcal mol^{-1} lower than corresponding values measured for the rearrangement of **IS** (AOH = H_2O; BE = 10 kcal mol^{-1}); (ii) the activation entropies for the **IS** → **C** or **B** rearrangements are invariably less negative than those concerning the **IS′** → **C^{I}** or **B^{I}** and the **IIR′** → **C^{II}** or **B^{II}** ones; (iii) compared to that measured for **IS**, no distinct differences in the activation energies and entropies were observed in the formation of **B**- and **C**-type complexes from **IS′** and **IIR′**.

Concerning points i and ii, a plausible explanation of the inverse BE vs $\Delta H^{\ddagger}$'s for the oxonium ions of Table 5 may be found by considering that $\Delta H^{\ddagger}$'s reflect the energy balance between the extent of C−O bond cleavage and the C−H···O interactions in the corresponding transition structures, which in turn, determines the position of the transition structure along the reaction coordinate. Previous studies of the thermochemistry of association of carbocations with n-donors demonstrated that the C−H···O interaction energy in hydrogen-bonded clusters between carbenium ions and n-donors is rather insensitive of the nature of both the ion and the donor.[34] For instance, the C−H···O interaction energy between oxocarbonium ions, such as $CH_3CH^+OCH_3$, and AOH (A = H or CH_3) increases by only 1.9 kcal mol^{-1} in passing from H_2O (11.2 kcal mol^{-1}) to the more nucleophilic and more polarizable CH_3OH (13.1 kcal mol^{-1}), whereas it remains virtually unaffected by varying the structure and stability of the oxocarbonium ion, i.e., $H_2O/CH_3CH^+OCH_3$ (11.2 kcal mol^{-1}) vs $H_2O/(CH_3)_2C^+OCH_3$ (10.8 kcal mol^{-1}).[35] If the hydrogen-bonded complexes involved in the rearrangement of the oxonium intermediates of Table 5 are characterized by comparable C−H···O interaction energies, some indication on the relative location of the corresponding transition structures along the reaction coordinate can be inferred from the following considerations.

Unimolecular rearrangement of O-protonated unsubstituted allylic alcohol **I** (AOH = H_2O; BE = 23.6 kcal mol^{-1})[1] proceeds through the corresponding **C**-type and **B**-type complexes, whose C−H···O interaction energies range from 13 to 15 kcal mol^{-1}.[1] The **I** → **C**-type and **I** → **B**-type rearrangements involve transition structures lying 11.8 and 10.9 kcal mol^{-1} above **I**, respectively, namely at energies very close to those of the complexes themselves, i.e., 10.5 and 8.3 kcal mol^{-1} above **I**, respectively. Therefore, the transition structure **I$_C$**‡ (and **I$_B$**‡) involved in the **I** → **C**-type (and **I** → **B**-type) rearrangement should be product-like and situated rather late along the relevant reaction coordinate. If the same C−H···O interaction energies (ca. 13−15 kcal mol^{-1}) operate in the **C** and **B** complexes, involved in the rearrangement of **IS** (AOH = H_2O; BE = 10 kcal mol^{-1}),[1] the energies of **C** and **B** are calculated around 3−5 kcal mol^{-1} *below* that of their oxonium precursor. This means that, relative to **I$_C$**‡ (and **I$_B$**‡), the transition structure **IS$_C$**‡ (and **IS$_B$**‡) involved in the **IS** → **C** (and **IS** → **B**) rearrangement should be more reactant-like and placed quite early along the relevant reaction coordinate. Furthermore, if the same C−H···O interaction energies (ca. 13−15 kcal mol^{-1}) operate also in the **C^{I}**, **C^{II}** and **B^{I}**=**B^{II}** complexes, involved in the rearrangement of **IS′** and **IIR′** (AOH = CH_3OH; BE = 19 kcal mol^{-1}), their energy is placed ca. 4−6 kcal mol^{-1} *above* that of the corresponding oxonium precursors. This implies that, relative to **I$_C$**‡ (and **I$_B$**‡), the transition structure **IS′$_C$**‡ (and **IS′$_B$**‡), involved in the **IS′** → **C^{I}** (or **IS′** → **B^{I}**) rearrangement, as well as the **IIR′$_C$**‡ (and **IIR′$_B$**‡) one, involved in the **IIR′** → **C^{II}** (**IIR′** → **B^{II}**) process, should be more product-like and located later along the relevant reaction coordinate.

This suggests that the activation energy of the **IS** → **C** and **IS** → **B** rearrangements reflects the limited elongation of the relatively weak C−OH_2 bond, without any significant energy compensation from the hydrogen-bond interactions between H_2O and a still rather flexible allylic residue. Instead, the lower activation energies of the **IS′** → **C^{I}** (or **IIR′** → **C^{II}**) and **IS′** → **B^{I}**=**B^{II}** ← **IIR′** rearrangements reflect the much more intense hydrogen-bond interactions between CH_3OH and the essentially planar allylic residue, necessary for counterbalancing the substantial energy required for the extensive C−O(H)-CH_3 bond fission. This view is also consistent with the $\Delta S^{\ddagger}$ values of Table 5. The tight transition structures involved in the **IS′** → **C^{I}** (or **IIR′** → **C^{II}**) and **IS′** → **B^{I}**=**B^{II}** ← **IIR′** rearrangements, characterized by an essentially planar 1-methyl-3-ethylallyl cationic moiety strongly orienting the CH_3OH molecule between its hydrogens, conform to the rather low values of $\Delta S^{\ddagger}$ ($-\Delta S^{\ddagger}$ = 11.2−14.6 cal mol^{-1} K^{-1}). The appreciably higher $\Delta S^{\ddagger}$ values

(34) Meot-Ner (Mautner), M.; Karpas, Z.; Deakyne, C. *J. Am. Chem. Soc.* **1986**, *108*, 3913. See also: (a) Audier, H. E.; Koyanagi, G. K.; McMahon, T. B.; Tholmann, D. *J. Phys. Chem.* **1996**, *100*, 8220. (b) Uggerud, E. *J. Am. Chem. Soc.* **1994**, *116*, 6873.

(35) Meot-Ner (Mautner), M.; Ross, M. M.; Campane, J. E. *J. Am. Chem. Soc.* **1985**, *107*, 4839.

Table 5. Arrhenius Parameters for the Gas-Phase Racemization and Regioisomerization of IS′, IIR′, and IS

process	BE(C−O)[a] (kcal mol^{-1})	Arrhenius equation[b]	r	$\Delta H^{\ddagger}$ (kcal mol^{-1}}	$\Delta S^{\ddagger}$ (cal mol^{-1} K^{-1})
IS′ → C^{I}	19	$\log k_{C^{I}} = (10.1 \pm 0.4) - (6.3 \pm 0.5)x$	0.960	5.6 ± 0.5	-14.6 ± 2.1
IS′ → B^{I}	19	$\log k_{B^{I}} = (10.6 \pm 0.4) - (5.4 \pm 0.5)x$	0.978	4.7 ± 0.5	-12.4 ± 2.1
IIR′ → C^{II}	19	$\log k_{C^{II}} = (10.3 \pm 0.4) - (6.5 \pm 0.6)x$	0.988	5.8 ± 0.6	-13.6 ± 2.1
IIR′ → B^{II}	19	$\log k_{B^{II}} = (10.9 \pm 0.4) - (5.8 \pm 0.5)x$	0.987	5.1 ± 0.5	-11.2 ± 1.9
IS → C	10	$\log k_{C} = (12.5 \pm 0.4) - (8.7 \pm 0.6)x$	0.963	8.0 ± 0.6	-3.7 ± 2.8
IS → B	10	$\log k_{B} = (11.6 \pm 0.4) - (7.4 \pm 0.5)x$	0.960	6.7 ± 0.5	-7.9 ± 2.4

[a] See refs 1 and 29. [b] $x = 1000/2.303RT$, R in cal mol^{-1} K^{-1}.

($-\Delta S^{\ddagger} = 3.7-7.9$ cal mol^{-1} K^{-1}), measured for the **IS → C** and **IS → B** rearrangements, reflect comparatively loose transition structures, wherein a flexible 1-methyl-3-ethylallyl moiety is only weakly bound to a more freely moving H_2O molecule.

Finally, taking into account the equal thermodynamic stability of the **IS′**−**IR′** and **IIS′**−**IIR′** oxonium racemates, the coincidence of the activation parameters for the **IS′ → B^{I}=B^{II} ← IIR′** rearrangements (point iii) represents a crucial test of the soundness of the kinetic methodology adopted. In addition, coincidence of the activation parameters for the **IS′ → C^{I}** and **IIR′ → C^{II}** racemizations comes up with the expectation of small energy differences in the corresponding transition structures, owing to comparable stability of their *endo*-ethyl-*exo*-methylallyl and *exo*-ethyl-*endo*-methylallyl moieties.

Conclusions

The kinetics and the mechanism of the acid-induced racemization and regioisomerization of (*S*)-*trans*-4-hexen-3-ol (**1S**) or (*R*)-*trans*-3-hexen-2-ol (**2R**) are investigated in the gas phase at pressures high enough to allow complete thermalization of all the reaction intermediates. The experimental methodology used, based on the radiolytic preparation of the acid catalyst, its attack on the allylic substrate in the presence of defined concentrations of a base, and the stereochemical identification of the neutral products, provides unequivocal evidence on the intramolecular nature of the racemization and regioisomerization processes, which proceed through distinct hydrogen-bonded complexes. The rate constants for their formation from the $(CH_3)_2Cl^+$-methylation of (*S*)-*trans*-4-hexen-3-ol (**1S**) or (*R*)-*trans*-3-hexen-2-ol (**2R**) are measured in the 40−120 °C temperature range and the relevant activation parameters derived from the analysis of the corresponding Arrhenius plots. Their comparison with the activation parameters concerning the proton-induced racemization and regioisomerization of (*S*)-*trans*-4-hexen-3-ol (**1S**), measured in previous gas-phase studies,[1] reveals that the energy, the charge distribution, and the position along the reaction coordinate of the relevant transition structures significantly depend on the nature of the moving moiety (AOH; A = H or CH_3). Thus, the racemization and regioisomerization of O-protonated (*S*)-*trans*-4-hexen-3-ol (**IS**) (AOH = H_2O) involve transition structures located early along the reaction coordinate. Instead, the transition structures involved the racemization and regioisomerization of O-methylated (*S*)-*trans*-4-hexen-3-ol (**IS′**) and (*R*)-*trans*-3-hexen-2-ol (**IIR′**) are placed later along the reaction coordinate and are characterized by a strong coordination of the moving moiety AOH = CH_3OH with the hydrogens of the allylic moiety. This gas-phase study provides a first comparative analysis of the intrinsic factors governing acid-catalyzed racemization of optically active alcohols, such as the nature and energetics of the involved ion−dipole pairs, the motion of the AOH molecule within the ion−dipole complexes, etc., whose identification is strongly complicated in solution by the action of the bulk solvent and of the counterion.

Acknowledgment. This research was supported by the Italian Ministero dell'Università e della Ricerca Scientifica e Tecnologica (MURST). We thank F. Gasparrini for his continuous encouragement and precious assistance in the preparation of the starting alcohols and the kinetic resolution of their racemates.

JO971282X